Inorg. Chem. **2007**, *46*, 2877−2882

Ternary Zirconium Tin Antimonide $ZrSn_{2-x}Sb_x$ ($0.2 < x < 0.8$), Different from the Parent Binaries $ZrSn_2$ and $ZrSb_2$

Andriy V. Tkachuk, Davin G. Piercey, and Arthur Mar*

Department of Chemistry, University of Alberta, Edmonton, Alberta, Canada T6G 2G2

Received November 30, 2006

The new intermetallic phase $ZrSn_{2-x}Sb_x$ was prepared by arc-melting and annealing at 800 °C. It adopts the hexagonal $CrSi_2$-type structure (Pearson symbol *hP*9, space group $P6_222$ (or $P6_422$), $Z = 3$, $a = 5.51$–5.53 Å, $c = 7.65$–7.63 Å) and exhibits a significant phase width ($0.2 < x < 0.8$). In contrast, the parent binary phases adopt different structures: $ZrSn_2$ has the orthorhombic $TiSi_2$-type structure, and $ZrSb_2$ exists as two orthorhombic forms (α-$ZrSb_2$, own type; "β-$ZrSb_2$", $PbCl_2$-type). The structures of $ZrSn_2$, $ZrSn_{2-x}Sb_x$, and β-$ZrSb_2$ are distinguished by the stacking and distortion of nets with composition "ZrQ_2" (Q = Sn, Sb). The $CrSi_2$-type and $TiSi_2$-type structures differ only minimally in energy, but interlayer Sb–Sb bonding is important in stabilizing the structure of β-$ZrSb_2$.

Introduction

Solid-state compounds containing mixed anions are less well understood than those containing mixed cations. The tendency for the anions to order depends on their size and charge,[1] but these guidelines have questionable applicability when the anionic components come from the heavier p-block elements. Counterintuitive examples are found in the ternary (Ti, Zr, Hf)−(Si, Ge, Sn)−Sb systems, where the rather chemically different Si and Sb atoms are partially disordered in $Ti_5Si_{1.3}Sb_{1.7}$ and $ZrSi_{0.7}Sb_{1.3}$,[2,3] whereas the similar Sn and Sb atoms are ordered in TiSnSb.[4] Moreover, there is the possibility that entropy may play an important role in stabilizing mixed-anion compounds characterized by differential fractional site occupancy (DFSO), just as in mixed-cation compounds.[5]

Several ternary phases, including anionic DFSO-stabilized compounds, have been identified in the quasibinary $ZrSi_2$−$ZrSb_2$ and $ZrGe_2$−$ZrSb_2$ systems. These include $ZrSi_{0.7}Sb_{1.3}$ and ZrGeSb (Cu_2Sb-type, also called PbFCl-type) at one end,[3] and $ZrSi_{0.1}Sb_{1.9}$ and $ZrGe_{0.2}Sb_{1.8}$ ($PbCl_2$-type, also called TiNiSi-type) at the other end.[6] The latter are isostructural to what was previously believed to be the binary phase β-$ZrSb_2$,[7,8] which seems to require small amounts of the tetrel component to be formed.[6] This conclusion also applies to the $ZrSn_2$−$ZrSb_2$ system, where a similar ternary $PbCl_2$-type compound $ZrSn_{0.4}Sb_{1.6}$ was found.[3]

A renewed investigation of the Sn-containing system seems worthwhile because the chemical similarity of Sn and Sb (in contrast to Si or Ge vs Sb) allows us to focus on the effect of electron count on the evolution of structure types in this series. This systematic study reveals the existence of a Sn-rich phase $ZrSn_{2-x}Sb_x$ adopting a different structure than those of the parent binary phases $ZrSn_2$ or $ZrSb_2$.

Experimental Section

Synthesis. Crystals of $ZrSn_{2-x}Sb_x$ ($x = 1.2$−1.3) were originally discovered as a byproduct from a reaction of a 0.25-g mixture of Th, Zr, and Sb powders in a 3:1:5 molar ratio in the presence of a 10-fold excess of Sn in an attempt to prepare Th_3ZrSb_5. The reactants were placed in an alumina crucible and sealed within an evacuated fused-silica tube. The tube was heated at 800 °C for 5 days and allowed to cool to room temperature after the furnace was turned off. To determine the phase width, samples of nominal composition $ZrSn_{2-x}Sb_x$ over $0 < x < 2$ in increments of 0.1 were subsequently prepared. Starting materials were elements of high purity (99.9% or better) in the form of zirconium wire, tin shot, and antimony rod. Mixtures of these elements were melted under an argon atmosphere in an Edmund Bühler MAM-1 compact arc melter, with 2.5 wt % excess of Sb added to compensate for evaporative loss. The ingots were then sealed in evacuated fused-silica tubes and annealed at 800 °C for 10 days. After the heat treatment, the ingots were quenched in cold water.

* To whom correspondence should be addressed. E-mail: arthur.mar@ualberta.ca.

(1) Fuertes, A. *Inorg. Chem.* **2006**, *45*, 9640−9642.
(2) Kleinke, H. *Can. J. Chem.* **2001**, *79*, 1338−1343.
(3) Lam, R.; Mar, A. *J. Solid State Chem.* **1997**, *134*, 388−394.
(4) Dashjav, E.; Kleinke, H. *J. Solid State Chem.* **2003**, *176*, 329−337.
(5) Franzen, H. F.; Köckerling, M. *Prog. Solid State Chem.* **1995**, *23*, 265−289.
(6) Soheilnia, N.; Assoud, A.; Kleinke, H. *Inorg. Chem.* **2003**, *42*, 7319−7325.
(7) Garcia, E.; Corbett, J. D. *J. Solid State Chem.* **1988**, *73*, 440−451.
(8) Garcia, E.; Corbett, J. D. *J. Solid State Chem.* **1988**, *73*, 452−467.

10.1021/ic062277r CCC: $37.00 © 2007 American Chemical Society
Published on Web 02/13/2007

Phase compositions were determined by powder X-ray diffraction (XRD) on an Inel powder diffractometer (Cu $K\alpha_1$ radiation) equipped with a CPS 120 detector and by energy-dispersive X-ray (EDX) analyses on a Hitachi S-2700 scanning electron microscope. In the range $0.2 < x < 0.8$, powder XRD patterns revealed single-phase product with the $CrSi_2$-type structure. EDX analyses on polished samples of the annealed ingots indicated elemental compositions consistent with the loaded stoichiometries ($ZrSn_{1.8}Sb_{0.2}$, expected 33% Zr, 60% Sn, 7% Sb, observed 28% Zr, 64% Sn, 8% Sb; $ZrSn_{1.2}Sb_{0.8}$, expected 33% Zr, 40% Sn, 27% Sb, observed 29% Zr, 44% Sn, 27% Sb). SEM images of these polished samples revealed a high degree of homogeneity consistent with single-phase product in the range $0.2 < x < 0.8$, in contrast to the phase segregation that was discernible in two-phase samples beyond this range.

Structure Determination. Single-crystal X-ray intensity data were collected for two crystals with nominal compositions (as determined by EDX analyses) of $ZrSn_{1.3}Sb_{0.7}$ and $ZrSn_{1.2}Sb_{0.8}$ on a Bruker Platform/SMART 1000 CCD diffractometer at 22 °C using ω scans. Structure solution and refinement were carried out with use of the SHELXTL (version 6.12) program package.[9] Face-indexed numerical absorption corrections were applied. Direct methods revealed atomic positions consistent with $CrSi_2$ and other isostructural metal disilicides, whose structure was originally refined in space group $P6_222$.[10] With only two crystallographically unique sites in this structure, site 3*c* (1/2, 0, 0) was occupied by Zr atoms whereas site 6*i* (*x*, 2*x*, 0) was constrained to be fully occupied by a mixture of Sn and Sb atoms in the proportions found from the EDX analyses. Given their similar scattering factors, any attempts to refine the occupancies of Sn and Sb in this site would prove futile. Because $P6_222$ is a non-centrosymmetric space group, the absolute structure should be determined. However, attempts to refine the Flack parameter resulted in values with uncertainties (1.0(0.6) for $ZrSn_{1.3}Sb_{0.7}$ and 0.7(0.6) for $ZrSn_{1.2}Sb_{0.8}$) too large for any conclusions to be drawn about the absolute structure, probably because of the low anomalous dispersion at this wavelength and the insufficient numbers of Friedel pairs available. Nevertheless, these values suggest a weak preference for the inverted structure, so the structure was subsequently refined in the enantiomorphous space group $P6_422$. The displacement ellipsoids are slightly oblate, being more flattened along the *c* direction, but this feature may be more likely an artifact of absorption correction than indicative of any real bonding anisotropies. Full crystallographic details, in the form of a CIF, are available as Supporting Information or may be obtained from Fachinformationszentrum Karlsruhe, Germany (No. CSD-417608 and CSD-417609).

Powder XRD data were also collected over 12 h on an Inel powder diffractometer for $ZrSn_{1.6}Sb_{0.4}$, and refinements were carried out with the full-profile Rietveld method using the program LHPM-Rietica.[11] Initial positions were taken from the single-crystal structure determined above. The final cycle of least-squares refinement included scale factor, background, zero point, cell parameters, pseudo-Voigt peak profile parameters, atomic coordinates, and isotropic displacement parameters. The fit of the Rietveld refinement results to the powder pattern is shown in Figure 1. Additional Rietveld refinements were performed on samples representing the endpoints of the homogeneity range of $ZrSn_{2-x}Sb_x$ ($0.2 < x < 0.8$), confirming that these were also single phases (Figure S1 in Supporting Information).

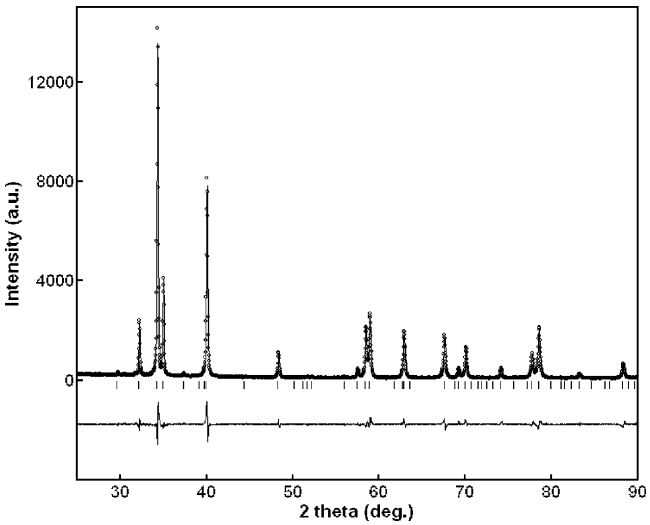

Figure 1. Rietveld refinement results for $ZrSn_{1.6}Sb_{0.4}$. The observed profile is indicated by circles and the calculated profile by the solid line. Bragg peak positions are located by the vertical tick marks. The difference plot is shown at the bottom.

Crystal data and further details of the data collections are given in Table 1. Interatomic distances are listed in Table 2.

Magnetic Measurements. Magnetic susceptibility measurements from 2 to 300 K were made on ground samples (~80−90 mg) of the end-members of $ZrSn_{2-x}Sb_x$ ($0.2 < x < 0.8$) on a Quantum Design 9T-PPMS dc magnetometer/ac susceptometer. The susceptibility was corrected for contributions for the holder diamagnetism and the underlying sample diamagnetism. Plots of the magnetic susceptibility data are shown in Figure S2 in the Supporting Information.

Band Structure. Tight-binding extended Hückel band structure calculations were performed using the EHMACC suite of programs.[12,13] Models considered were $ZrSn_2$ and $ZrSb_2$ with idealized $TiSi_2$-type, $CrSi_2$-type, or $PbCl_2$-type structures,[14] and properties were extracted from the band structure using at least ~100 *k*-points in the irreducible portion of the Brillouin zone. The atomic parameters (valence shell ionization potentials H_{ii} (eV) and orbital exponents ζ_i) were as follows. For Zr 5s, $H_{ii} = -8.52$, $\zeta_i = 1.82$; for Zr 5p, $H_{ii} = -4.92$, $\zeta_i = 1.78$; for Zr 4d, $H_{ii} = -8.63$, $\zeta_{i1} = 3.84$, $c_1 = 0.621$, $\zeta_{i2} = 1.51$, $c_2 = 0.580$; for Sn 5s, $H_{ii} = -16.16$, $\zeta_i = 2.12$; for Sn 5p, $H_{ii} = -8.32$, $\zeta_i = 1.82$; for Sb 5s, $H_{ii} = -18.80$, $\zeta_i = 2.32$; for Sb 5p, $H_{ii} = -11.70$, $\zeta_i = 2.00$. The band structure of $ZrSn_2$ with a hypothetical $CrSi_2$-type structure was also calculated with the Stuttgart TB-LMTO program in which density functional theory is applied using the local density and atomic spheres approximations.[15] The conclusions drawn by analyzing the DOS and COHP curves from the LMTO calculations are similar to those from the extended Hückel calculations, so only the latter are reported.

Results and Discussion

Phase relations in the quasibinary $ZrSn_2-ZrSb_2$ system at 800 °C have been investigated in this study. Given the

(9) Sheldrick, G. M. *SHELXTL*, version 6.12; Bruker AXS Inc.: Madison, WI, 2001.
(10) Tanaka, K.; Nawata, K.; Inui, H.; Yamaguchi, M.; Koiwa, M. *Intermetallics* **2001**, *9*, 603−607.
(11) Hunter, B. *LHPM−Rietica*, version 1.7.7; International Union of Crystallography Commission on Powder Diffraction Newsletter, no. 20 (summer), 1998 (www.rietica.org).
(12) Whangbo, M.−H.; Hoffmann, R. *J. Am. Chem. Soc.* **1978**, *100*, 6093−6098.
(13) Hoffmann, R. *Solids and Surfaces: A Chemist's View of Bonding in Extended Structures*; VCH Publishers: New York, 1988.
(14) Villars, P., Ed. *Pearson's Handbook, Desk Edition*; ASM International: Materials Park, OH, 1997.

Table 1. Crystallographic Data for $ZrSn_{2-x}Sb_x$ ($x = 0.4, 0.7, 0.8$)

formula	$ZrSn_{1.6}Sb_{0.4}$	$ZrSn_{1.3}Sb_{0.7}$	$ZrSn_{1.2}Sb_{0.8}$
fw	329.82	330.74	331.05
space group	$P6_222/P6_422$ (No. 180/181)	$P6_222/P6_422$ (No. 180/181)	$P6_222/P6_422$ (No. 180/181)
T (°C)	295	295	295
a (Å)	5.5229(2)	5.5142(4)	5.5156(6)
c (Å)	7.6470(2)	7.6287(6)	7.6259(9)
V (Å^3)	202.00(1)	200.88(3)	200.91(4)
Z	3	3	3
x_Q[a]	0.1629(4)	0.16699(3)	0.16706(3)
ρ_{calcd} (g cm^{-3})	8.130	8.202	8.208
radiation	Cu Kα_1, $\lambda = 1.54056$ Å	Mo Kα, $\lambda = 0.71073$ Å	Mo Kα, $\lambda = 0.71073$ Å
μ (cm^{-1})	221.2	224.7	225.44
2θ range	15.0−90.0°	8.5−66.0°	8.5−66.0°
no. of data collected	2586	2734	2662
no. of unique data	58 Bragg reflections	263 (238 with $F^2 > 2\sigma(F^2)$)	264 (258 with $F^2 > 2\sigma(F^2)$)
no. of variables	19	10	11
residuals[b]	$R_B = 0.021$ $R_p = 0.084$ $R_{wp} = 0.106$	$R(F)$ ($F^2 > 2\sigma(F^2)$) $= 0.034$ $R_w(F^2) = 0.086$	$R(F)$ ($F^2 > 2\sigma(F^2)$) $= 0.026$ $R_w(F^2) = 0.094$
GOF, χ^2	3.30	1.47	1.74

[a] Atomic positions: Zr at 3*c* (1/2, 0, 0), *Q* at 6*i* (x_Q, 2x_Q, 0) where Q = Sn or Sb. [b] $R_B = \sum|I_o - I_c|/\sum I_o$; $R_p = \sum|y_o - y_c|/\sum y_o$; $R_{wp} = [\sum [w(y_o - y_c)]/\sum wy_o^2]^{1/2}$; $R(F) = \sum||F_o| - |F_c||/\sum|F_o|$; $R_w(F_o^2) = [\sum[w(F_o^2 - F_c^2)^2]/\sum wF_o^4\ ]^{1/2}$, $w^{-1} = [\sigma^2(F_o^2) + (Ap)^2 + Bp]$ where $p = [\max(F_o^2,0) + 2F_c^2]/3$.

Table 2. Selected Interatomic Distances (Å) in $ZrSn_{2-x}Sb_x$ ($x = 0, 0.4, 0.7, 0.8, 2.0$)[a]

	$ZrSn_2$	$ZrSn_{1.6}Sb_{0.4}$	$ZrSn_{1.3}Sb_{0.7}$	$ZrSn_{1.2}Sb_{0.8}$	β-$ZrSb_2$
			Intralayer		
Zr−*Q*	3.192 (× 2)	3.225(5) (× 2)	3.1805(3) (× 2)	3.1807(5) (× 2)	2.923(1)
	3.242 (× 4)	3.171(2) (× 4)	3.1852(3) (× 4)	3.1863(5) (× 4)	2.976(1) (× 2)
					3.060(1) (× 2)
					3.209(1)
Q−*Q*	3.242 (× 2)	3.225(5) (× 2)	3.1805(3) (× 2)	3.1807(5) (× 2)	3.146(1) (× 2)
	3.193	3.117(9)	3.1898(3)	3.1919(5)	3.849(1)
			Interlayer		
Zr−*Q*	2.964 (× 4)	3.016(1) (× 4)	2.9992(2) (× 4)	2.9985(3) (× 4)	3.032(1) (× 2)
					3.091(1)
Q−*Q*	2.965 (× 2)	2.988(2) (× 2)	3.0017(2) (× 2)	3.0014(3) (× 2)	2.890(1) (× 2)
					3.581(1) (× 2)
					3.731(1)
ref	16, 17	this work	this work	this work	8

[a] Q = Sn or Sb.

similar sizes of Sn and Sb, a reasonable expectation is that solid solutions should form. At the Sn-rich end of this system, the maximum solubility of Sb into $ZrSn_2$, which adopts the $TiSi_2$-type structure,[16,17] has been found to be less than 5%, corresponding to the composition $ZrSn_{1.9}Sb_{0.1}$. At the Sb-rich end, the maximum solubility of Sn into "β-$ZrSb_2$" with the $PbCl_2$-type structure[6−8] (also called TiNiSi-type) is 25%, corresponding to the composition $ZrSn_{0.5}Sb_{1.5}$. This result is consistent with earlier work in which $ZrSn_{0.4}Sb_{1.6}$ was obtained in the presence of excess Sn.[3] Moreover, the ready formation of these solid solutions contrasts with the problematic synthesis of pure "β-$ZrSb_2$", lending further support to the claim that the latter is really an impurity-stabilized ternary phase.[6] However, for ease of discussion, we shall treat "β-$ZrSb_2$" as if it were a true binary phase.

Intermediate regions of the $ZrSn_2$−$ZrSb_2$ system might then be expected to consist of two phases, $ZrSn_{1.9}Sb_{0.1}$ and $ZrSn_{0.5}Sb_{1.5}$. However, what really emerges is a new ternary intermetallic phase $ZrSn_{2-x}Sb_x$ adopting the hexagonal $CrSi_2$-type structure, which is different from either of the parent binaries. Compounds that adopt this structure type have been previously limited to early transition-metal disilicides MSi_2 or digermanides MGe_2 (M = V, Nb, Ta, Cr, Mo, W) and only one instance of a distannide, $HfSn_2$.[18] The new $ZrSn_{2-x}Sb_x$ phase represents the first ternary example of this structure type. The structure is densely packed by stacking slabs of 10-coordinate Zr-centered polyhedra along the *c* direction (Figure 2a). Each Zr atom is surrounded by a hexagonal waist of six *Q* atoms and pairs of *Q* atoms above and below (where Q = Sn or Sb) at distances of 3.0−3.2 Å (Figure 2b). If four more Zr atoms 3.75 Å away are considered (not shown), 14-coordination is attained, but these distances are too far to be significant. The coordination geometry and distances around the *Q* atoms are similar, except that five of the 10 nearest neighbors are now Zr atoms and the four more distant atoms are other *Q* atoms. Figure 3 shows that this phase is stable in the region $0.2 < x < 0.8$, with a trend toward increasing cell volume as more Sb is substituted into the structure at the expense of Sn. This cell expansion is not isotropic, since *c* actually decreases

(15) Tank, R.; Jepsen, O.; Burkhardt, A.; Andersen, O. K. *TB−LMTO−ASA program*, version 4.7; Max Planck Institut für Festkörperforschung: Stuttgart, 1998.
(16) Nowotny, H.; Schachner, H. *Monatsh. Chem.* **1953**, *84*, 169−180.
(17) Kwon, Y.−U.; Corbett, J. D. *Chem. Mater.* **1990**, *2*, 27−33.
(18) Villars, P., Ed. *Pauling File Binaries Edition*, version 1.0; ASM International: Materials Park, OH, 2002.

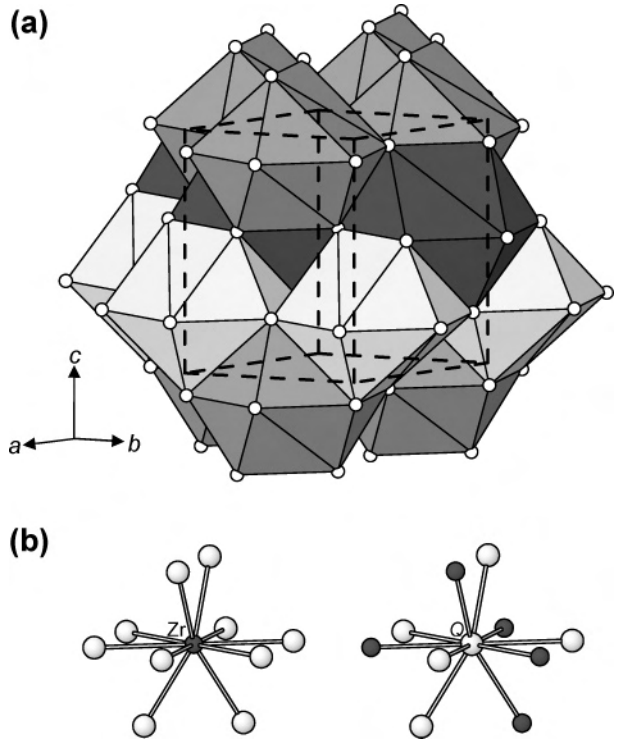

Figure 2. (a) Structure of $ZrSn_{2-x}Sb_x$ ($0.2 < x < 0.8$) in terms of Zr-centered polyhedra, arranged in slabs stacked along the *c* direction. (b) 10-coordinate polyhedra centered around the Zr (solid circles) and *Q* (Sn or Sb) atoms (open circles).

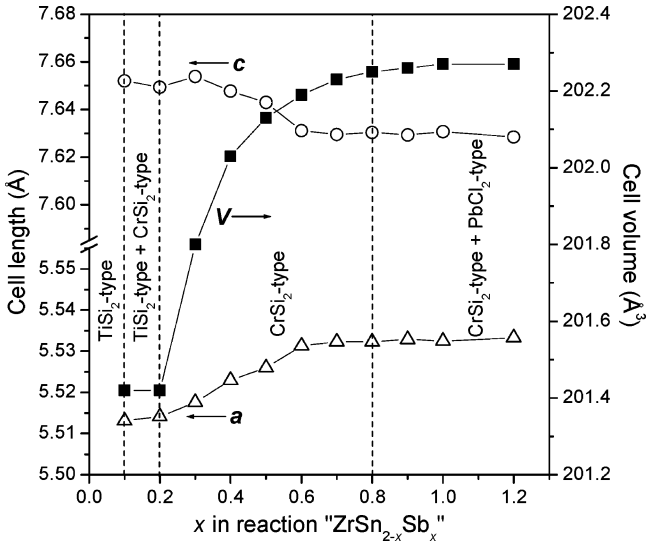

Figure 3. Plot of cell parameters vs *x* for $CrSi_2$-type phase observed in reactions with nominal composition $ZrSn_{2-x}Sb_x$. Regions of phase stability are $0 < x < 0.1$ for $TiSi_2$-type, $0.2 < x < 0.8$ for $CrSi_2$-type, and $1.5 < x < 2.0$ for $PbCl_2$-type. Elsewhere, two phases are present.

while *a* increases. Strictly speaking, the conditions for DFSO stabilization are not entirely satisfied because there is only one crystallographic site *Q* for the anions and the homogeneity range is large. This implies that electron count may be an important factor in stabilizing this phase.

The structures found in the $ZrSn_2-ZrSb_2$ system are compared in Figure 4. The description of the $TiSi_2$- and $CrSi_2$-type structures in terms of a layer stacking is conventional,[19] but it is unusual for the $PbCl_2$-type structure adopted by β-$ZrSb_2$, which is typically portrayed in terms of Zr-centered polyhedra.[6,8] In fact, all three structures exhibit strong bonding in three dimensions. However, this formalism serves to highlight the different stacking sequences of 3^6 layers, which in turn consist of interpenetrating 6^3 (hexagonal) nets of *Q* atoms and larger 3^6 (triangular) nets of Zr atoms. The structures are then distinguished by four-layer ($TiSi_2$-type, ABCD), three-layer ($CrSi_2$-type, ABC), and two-layer ($PbCl_2$-type, AB) sequences. Among transition-metal disilicides, the structure normally represented by the two-layer stacking would be the $MoSi_2$-type. In contrast, the layers in β-$ZrSb_2$ are highly buckled, associated with the formation of interlayer Sb−Sb bonds (depicted by thin lines in Figure 4c).

Band structure calculations were performed in an attempt to gain insight on the structural transitions in the $ZrSn_2-ZrSb_2$ system. At the Sn-rich end, total energy calculations show that $ZrSn_2$ is marginally more stable as the observed $TiSi_2$-type structure than a hypothetical $CrSi_2$-type structure by only 0.2 eV/f.u. (20 kJ/mol). At the Sb-rich end, $ZrSb_2$ is significantly more stable as the observed $PbCl_2$-type structure than a hypothetical $CrSi_2$-type structure by 3.9 eV/f.u. (370 kJ/mol). In the intermediate regime, however, the results are ambiguous. If a rigid band model is applied to mimic the effect of substituting Sn with Sb atoms, increasing the electron count in the band structures of $ZrSn_2$ modeled as either the $TiSi_2$-type or $CrSi_2$-type structures does not lead to any crossover in energy. In itself, this is not a surprising result because the local coordination environments in both structure types are essentially identical. Similar problems have been found in theoretical treatments of the structural transitions in the prototypic metal disilicides themselves ($TiSi_2$, $CrSi_2$, $MoSi_2$),[20−24] where the energy differences fall within the order of stacking fault energies. It has been suggested that these energy differences can be traced to $d\pi-p\pi$ bonding between the transition-metal and silicon atoms which would be sensitive to dihedral angles affected by different stacking sequences.[23] Such π-bonding seems less likely on proceeding to the heavier Sn or Sb atoms. Alternatively, entropy contributions may be responsible for the discrepancy in observed vs predicted structures, as has been invoked for the silicides.[23]

With the expectation that the band structure of $ZrSn_{2-x}Sb_x$ ($0.2 < x < 0.8$) should still resemble that of a hypothetical $ZrSn_2$ ($CrSi_2$-type) model, the DOS and COOP curves for the latter are shown in Figure 5. The DOS comprises a lower-energy Sn-based and a higher-energy Zr-based manifold of states. Experimentally, the end-members of $ZrSn_{2-x}Sb_x$ ($0.2 < x < 0.8$) were found to exhibit temperature-independent Pauli paramagnetism (Figure S2 in Supporting Information), with susceptibility values of 4.6×10^{-4} emu/mol for $ZrSn_{1.8}$-

(19) Pearson, W. B. *The Crystal Chemistry and Physics of Metals and Alloys*; Wiley: New York, 1972.
(20) Mattheiss, L. F. *Phys. Rev. B* **1991**, *43*, 12549−12555.
(21) Mattheiss, L. F. *Phys. Rev. B* **1992**, *45*, 3252−3259.
(22) Carlsson, A. E.; Meschter, P. J. *J. Mater. Res.* **1991**, *6*, 1512−1517.
(23) Pankhurst, D. A.; Nguyen−Manh, D.; Pettifor, D. G. *Phys. Rev. B* **2004**, *69*, 075113−1−075113−9.
(24) Colinet, C.; Wolf, W.; Podloucky, R.; Pasturel, A. *Appl. Phys. Lett.* **2005**, *87*, 041910−1−041910−3.

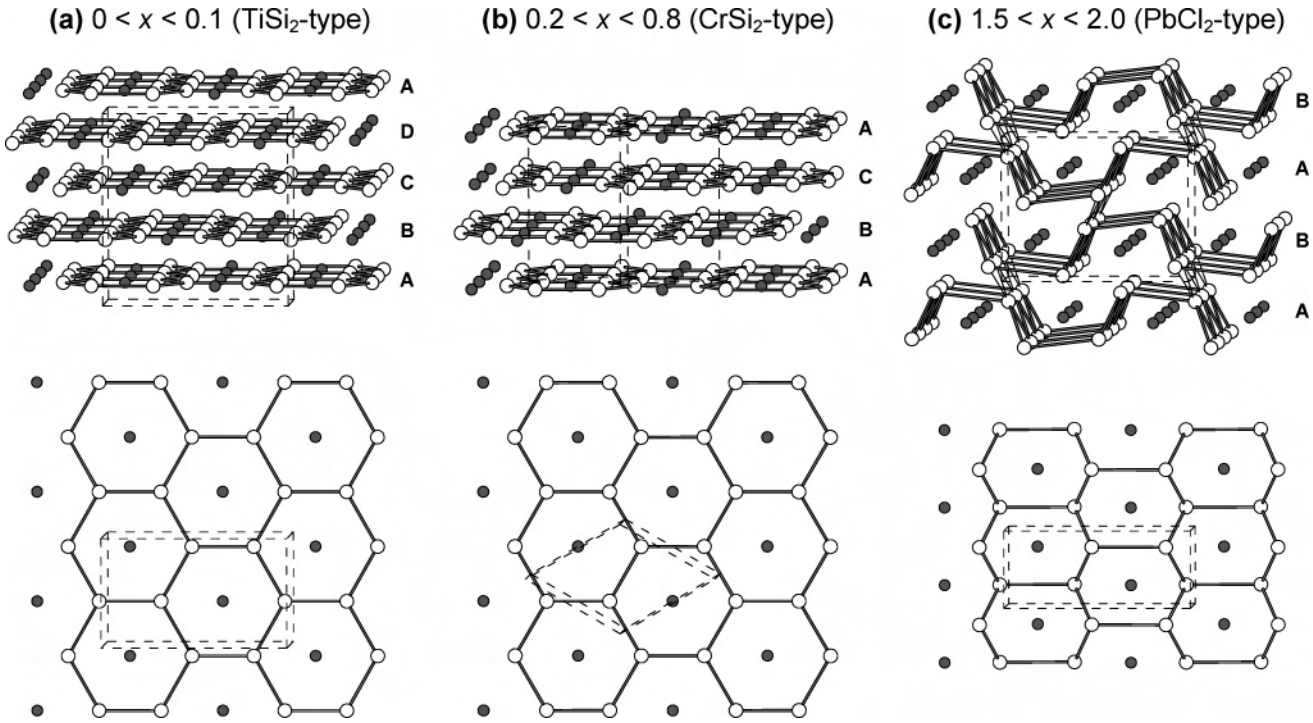

Figure 4. Evolution of structures in $ZrSn_{2-x}Sb_x$ for (a) $0 < x < 0.1$, (b) $0.2 < x < 0.8$, and (c) $1.5 < x < 2.0$ in terms of different stacking sequences of 3^6 nets. The solid circles are Zr atoms and the open circles are *Q* (Sn or Sb) atoms.

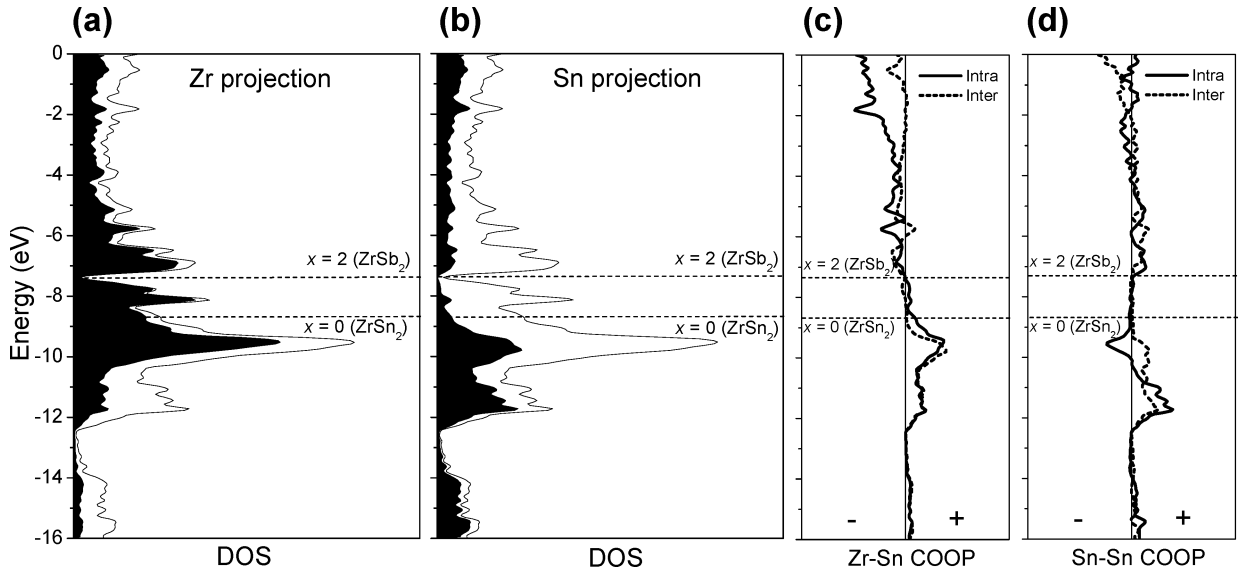

Figure 5. Contributions of (a) Zr and (b) Sn (shaded regions) to the total density of states (DOS) (line), and crystal orbital overlap population (COOP) curves for intralayer and interlayer (c) Zr−Sn and (d) Sn−Sn interactions in $ZrSn_2$ with a hypothetical $CrSi_2$-type structure. The Fermi levels corresponding to the electron count for $ZrSn_2$ and $ZrSb_2$ are marked by the horizontal lines.

$Sb_{0.2}$ and 4.0×10^{-4} emu/mol for $ZrSn_{1.2}Sb_{0.8}$. Consistent with this observation, the Fermi level crosses partially filled bands at all electron counts until $x = 2$ ($ZrSb_2$), where a small gap appears. This gap corresponds to the pseudogap observed at the Fermi level for the true band structure of β-$ZrSb_2$[6] and appears to be an artifact of the extended Hückel calculation. In the corresponding LMTO calculation for $ZrSn_2$ ($CrSi_2$-type), there is also only a pseudogap at this electron count and there is more mixing of Zr and Sn states near the Fermi level. Inspection of the COOP curves (Figure 5c and d) reveals that as the electron count increases from $x = 0$ to $x = 2$, the Zr−Sn states being filled are only weakly bonding and the Sn−Sn states are essentially nonbonding. The insensitivity of the bonding character, whether intralayer or interlayer, is consistent with the relatively large homogeneity range observed for $CrSi_2$-type $ZrSn_{2-x}Sb_x$ ($0.2 < x < 0.8$), but it does not explain the trend in the *a* and *c* parameters (Figure 3), which may arise from a combination of both electronic and size effects. Although Sn has a slightly larger metallic radius (1.42 Å) than Sb (1.39 Å),[25] it is also less electronegative. In a ternary compound, the differing degree of charge transfer to Sn vs Sb can render the metal−Sn bonds

(25) Pauling, L. *The Nature of the Chemical Bond*, 3rd ed.; Cornell University Press: Ithaca, NY, 1960.

shorter than the metal−Sb bonds, as observed in TiSnSb.[4] Moreover, because of the greater propensity for hypervalent Sb−Sb bonding compared to Sn−Sn bonding,[26] the increasing stabilization afforded by higher Sb concentrations drives the system to favor a structure with greater Sb−Sb bonding.

It seems clear that the structural transitions seen here are governed by electron count, but the effects are more subtle than in the prototypic disilicides MSi_2.[27] In the $ZrSn_2$−$ZrSb_2$ system, intermediate electron counts (VEC = 12.2−12.8) lead to a different structure type for $ZrSn_{2-x}Sb_x$ ($CrSi_2$-type). Extension of these studies to the $CrSn_2$−$CrSb_2$ system has revealed a ternary phase, $CrSn_{1.6}Sb_{0.4}$,[28] with a related Mg_2-Cu-type structure whose electron count (VEC = 14.4) exceeds those of known representatives among the distannides MSn_2.[29] Given that binary transition-metal stannides and antimonides generally do *not* adopt the same structure types, these results encourage us to examine mixed Sn−Sb systems further.

Acknowledgment. Acknowledgment is made to the Donors of the American Chemical Society Petroleum Research Fund for support of this research. We thank Dr. Robert McDonald and Dr. Michael J. Ferguson (X-ray Crystallography Laboratory) for the X-ray data collection and Ms. Christina Barker (Department of Chemical and Materials Engineering, University of Alberta) for assistance with the SEM-EDX analysis.

Supporting Information Available: One X-ray crystallographic file in CIF format and two figures showing additional Rietveld refinement results and plots of magnetic susceptibility data. This material is available free of charge via the Internet at http://pubs.acs.org.

IC062277R

(26) Ienco, A.; Hoffmann, R.; Papoian, G. *J. Am. Chem. Soc.* **2001**, *123*, 2317−2325.
(27) Jeitschko, W. *Acta Crystallogr. Sect. B* **1977**, *33*, 2347−2348.
(28) Crerar, S. J.; Mar, A. Unpublished results.
(29) Wölpl, T.; Jeitschko, W. *J. Alloys Compd.* **1994**, *210*, 185−190.